

## LOI Progress Report

— Looking for a new tuning method of the LOI —

June 4, 2012

### 1. Introduction

Thanks to the improvements on a grid switcher and the high power drive (HPD) cooling pipe, experiments could be performed very efficiently: no trips of grid switcher, and simultaneous operation of the LOI plus another two 2RF systems. A new digital master oscillator (MO) was available, which has a subharmonic content as low as -60dB. With this MO, new record of gap voltage was obtained at 8.4kVp with bias tuning loop using grid and gap voltages. However, in the experiment with beam at  $2.54 \times 10^{13}$  ppp, it was found that the grid voltage was strongly deformed by the subharmonic component of the beam itself. On the other hand, the grid input current was hardly affected by the beam, and still showed a fine sine waveform. Although this characteristic might be an advantage, it means in turn the grid input current is quite insensitive to the load conditions. A new LOI tuning system is then discussed in this report from view point of tuning sensitivity. Preliminary test on the beam loss with LOI and another two 2RF systems in parallel operation was also conducted.

In the following sections are described, experimental setup including the above improvements in section 2, experimental results in section 3, sensitivity analysis in section 4, buck regulator fault in section 5, and discussions & conclusions in section 6.

### 2. Experimental setup

#### 2.1 TDR measurement of cable length

For correct phase detection, it is essential to make the cable length equal for the relevant cables. Cable length was measured by the TDR 1000/2 (Time Domain Reflectometer, Megger limited) for the gap voltage, grid voltage, cavity input current and grid input current. The cable end was opened at the RF MCR end, and the measurement was performed from the LOI end. The results are shown in [fig. 1](#), where the relative velocity through cable was selected to be 0.66, or 5ns/m. However, it was found that the physical cable length differs from the measured one by 13~14% as shown in [Table 1](#). It seems as if the velocity is assumed faster by the same amount in the TDR. The reason of this difference was not clear. The delay time in the splitter is measured to be 17.2ns by the oscilloscope. If it is converted to the equivalent cable length, it amounts to 3.84m by using the same conversion factor, ie.  $v/c = 0.66 \times 1.13$ . Total length is then 131m for the gap volt, which is 1m longer than the others.

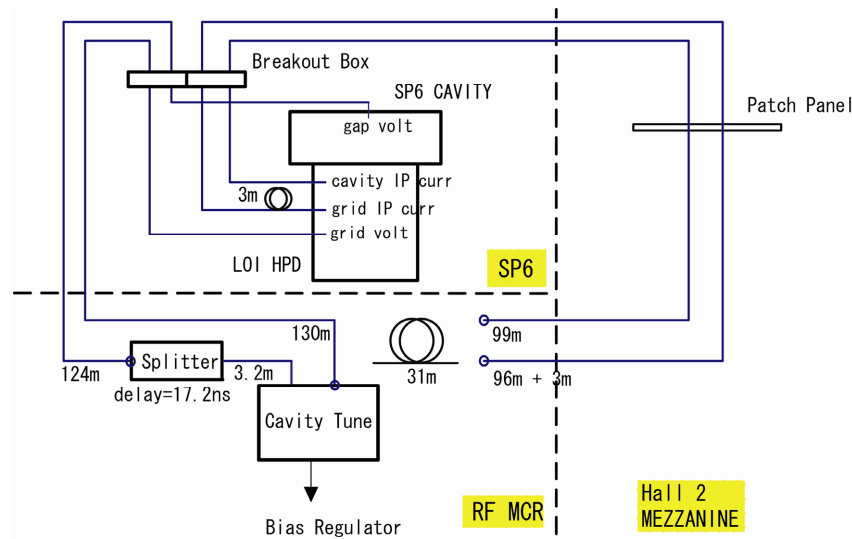


Fig. 1: Cable length measurement. Small circle at the cable end shows that this end was opened for TDR measurements. Numbers at the cable end stands for the measured values. 31m rolled cable is added to make 130m length for the cavity input current or the grid input current cable when it is used.

Table 1: Comparison of cable length for RG58 c/u LS2H ( $v/c = 0.66$ )

Physical length [m]	TDR measurement [m]	Difference
3.6	4.1	14%
37.2	42	13%

## 2.2 Grid switcher

Neil has redesigned the grid switcher to have fast turn-on and turn-off time of the switching IGBT, which enables fast transition from cut-off to a saturated mode or vice versa. Power dissipations in the IGBT switch are then made minimal. By a differential measurement between emitter and collector voltages, the turn-on time was confirmed to be 40ns as shown in fig. 2. Fig. 3 shows the photos before and after the modification. New circuit drawings are available at [http://www-accps.kek.jp/Low-Impedance\\_Cavity/gridswitcher\\_02.pdf](http://www-accps.kek.jp/Low-Impedance_Cavity/gridswitcher_02.pdf).

## 2.3 HPD cooling pipe

Cooling pipe from the water manifold to the LOI HPD, which is made of silicone NTS-braided hose, had an inner radius of 32mm and an excessive length of 6m. The pipe was replaced by a stainless-steel pipe of 38.1mm I.D. with the shortest length (fig. 4). Pipe conductance was then improved, and the water supply to the LOI and another two 2RF systems in parallel became possible.

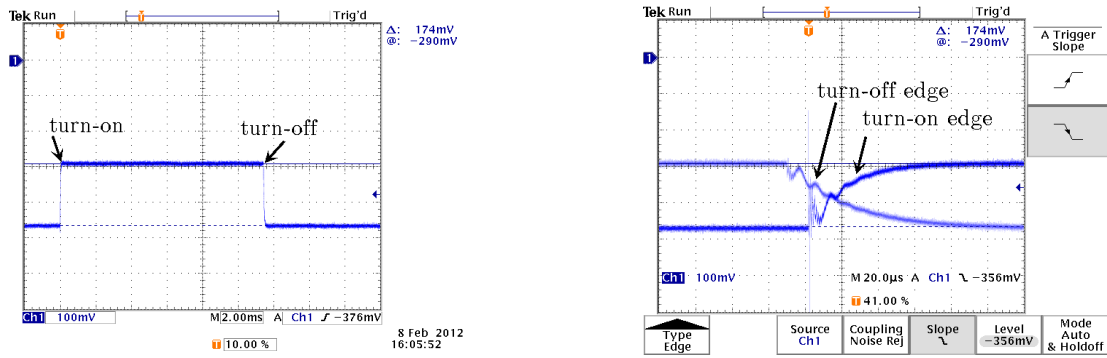


Fig. 2a: Grid switcher output voltage. Right figure show waveforms in a magnified scale.

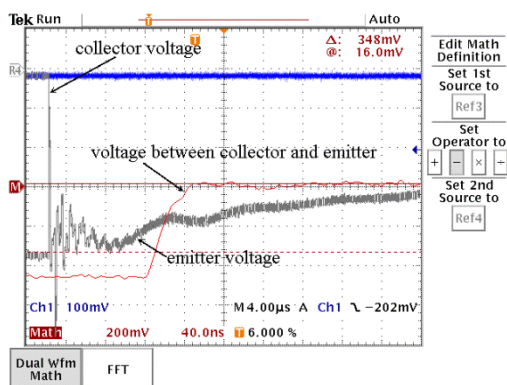


Fig. 2b: Differential voltage measurement (red) between collector and emitter voltage using the math function of oscilloscope.

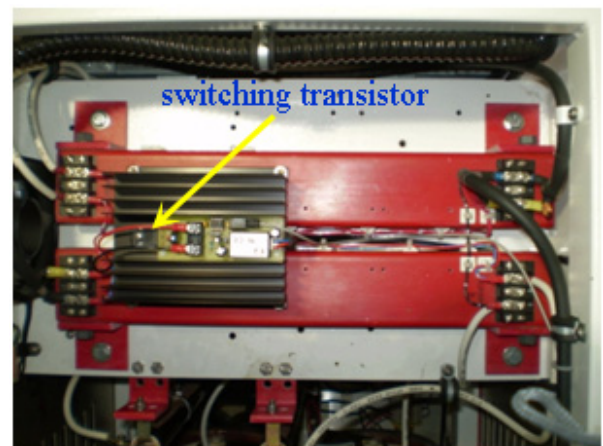
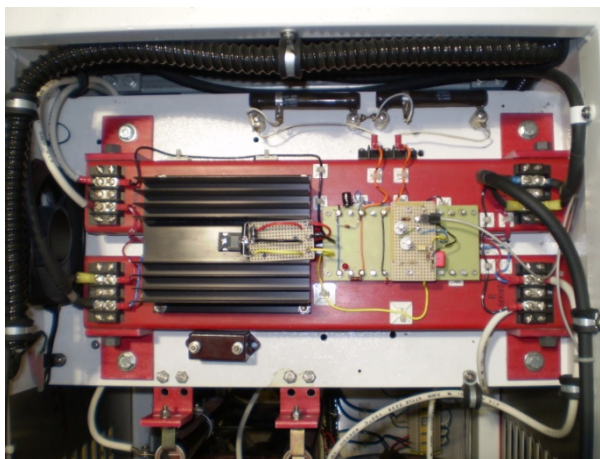


Fig. 3: Switching transistor and peripheral circuit board before (left) and after (right) improvement.



Fig. 4: HPD cooling manifold before (left) and after (right) replacement of cooling hose with stainless pipe.

### 3. Experimental results

#### 3-1 Cavity tuning and high RF voltage generation using a new digital master oscillator

The second subharmonic content is decreased to be -60dB by using the new digital master oscillator (MO) as shown in fig. 5. Fig. 6a shows the waveforms at 4.18ms, and their Fourier spectra in fig. 6b, where the cavity tuning was made by phase detection (PD) of the gap and grid voltages. It is seen in the figure subharmonic content (harmonic number = 1) is drastically reduced, although higher harmonic components are still large in the cavity input current and grid voltage. It can be thought these higher harmonics are generated in the subsequent stage such as in the solid-state amplifier or in the tetrode valve.



Fig. 5: Frequency spectra of the new digital MO (green) and the old one (yellow). Subharmonic peak locates at 1.4MHz (marker 1) and the 2RF spectrum ranges from 2.7 to 6.2MHz (between markers 2 and 3). The difference of amplitude between 1.4MHz and 2.7MHz components is -60dB for the new MO.

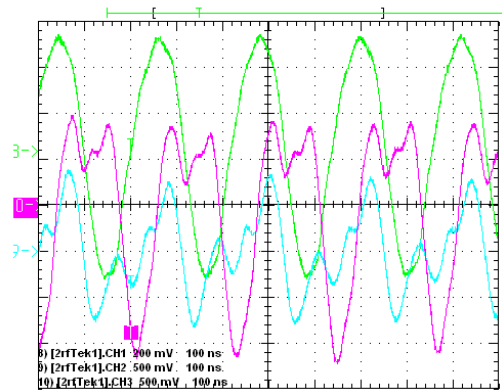


Fig. 6a: LOI operation at 6kV using a new digital MO. Waveforms at 4.182ms.  
 Ch1 (green): Triode Grid Input current  
 Ch2 (cyan): Cavity Input Current  
 Ch3 (magenta): Triode Grid Volts

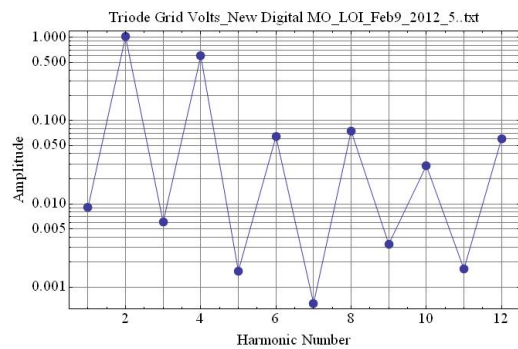
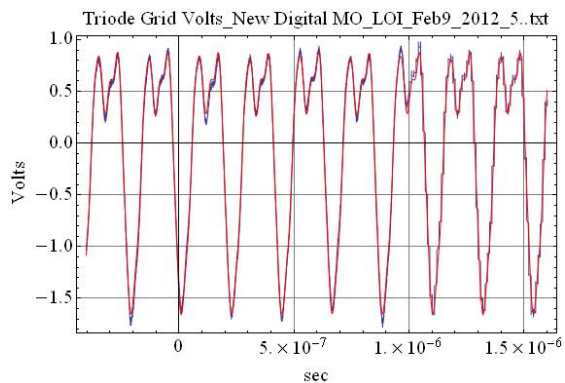
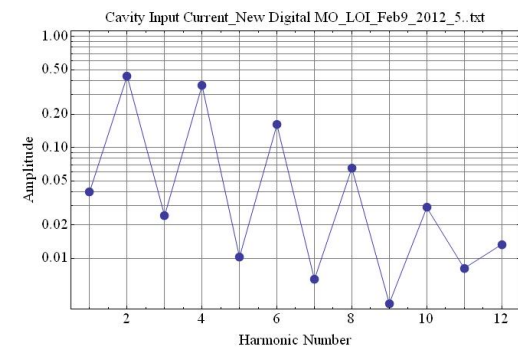
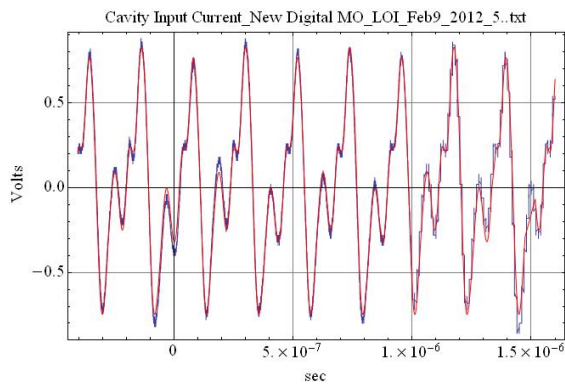
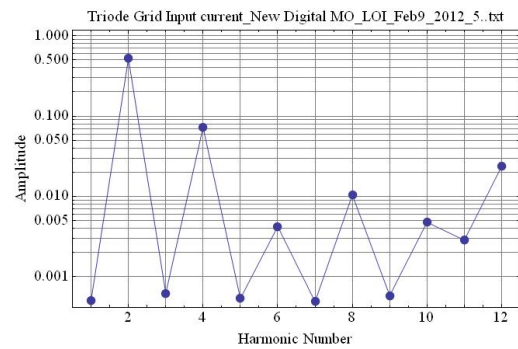
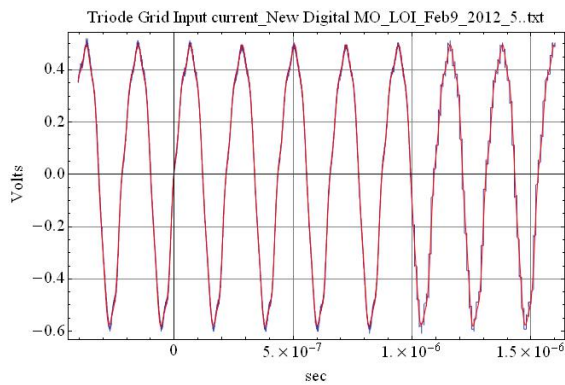


Fig. 6b: Fourier spectra of the waveforms in fig. 6a. From top, grid input current, cavity input current and grid voltage.

It was tried to produce as much high gap voltage as possible by using the digital MO. The new record of 8.4kVp was obtained at 1.85ms as shown in [fig. 7](#), where the tune correction was applied by a function input to minimize the buck regulator current ([fig. 8](#)). Even with the digital MO, phase detector output is still noisy at later half of the cycle, which will probably be due to the higher harmonic distortions in the grid voltage.

Although the digital MO produced a cleaner PD output than the old MO, it could not be used in the actual operation because the output frequency has an offset of  $\sim 30\text{kHz}$ . In the subsequent tests with beam, the old MO was then used.

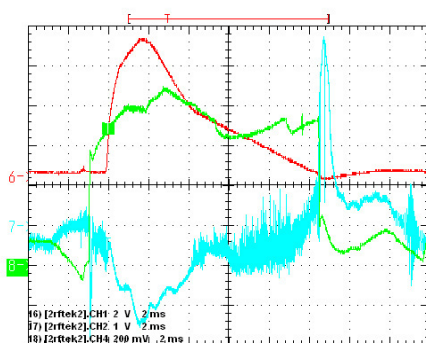


Fig. 7: LOI operation at 8.4kV using a new digital MO. PD was made using gap and grid voltages.  
Ch1 (red): LOI Gapvolts Envelope (1.2kV/V)  
Ch2 (cyan): Cavity Tune PD (1V=10degree)  
Ch4 (green): Buck Regulator Current (35A/V)

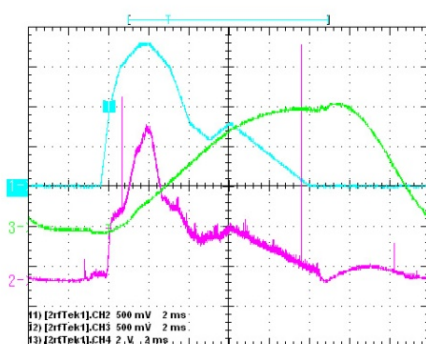


Fig. 8: LOI operation at 8.4kV using a new digital MO.  
Ch2 (cyan): Cavity Tune Correction Function  
Ch3 (magenta): Cavity Input Current (Via envelope detector)  
Ch4 (green): Output to Bias Regulator (corrected)

### 3-2 Waveform distortions by the beam

Waveforms of the grid voltage and grid input current were observed with beam, where the LOI, 2RF5 and 2RF8 were operated. The results were shown in [figs. 9 and 10](#) at 4.182ms after field minimum. Without beam, the grid voltage was already distorted by the subharmonic content of the old MO. With beam at  $2.54 \times 10^{13}$  ppp intensity, grid voltage became much more distorted. Thus, correct phase comparison is difficult with these waveforms. In contrast, grid input current shows a fine sine waveform even with beam, because the output impedance of the driver amplifier is so high that it acts as a constant

current source [1]. Fig. 11 shows the Fourier spectrum of the RF waveforms with and without the beam, and that of beam pulse.

The reason of the strong distortion on the grid voltage is thought to be the beam loading, which is discussed in the next section.

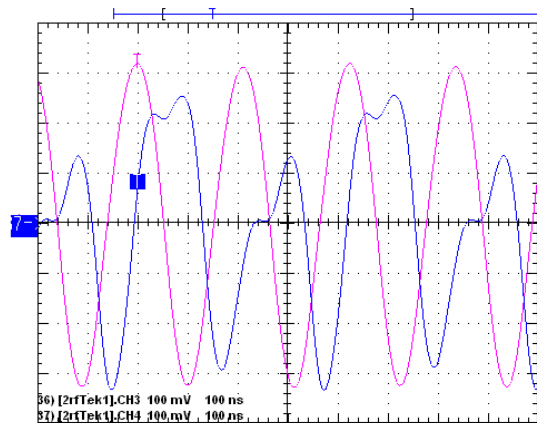


Fig. 9: LOI operation at 5.6kV using old MO. Beam on.  $2.54 \times 10^{13}$  injected,  $2.40 \times 10^{13}$  accelerated (99% acc. efficiency on good pulse!)

Ch3 (pink): LOI Grid Current Monitor averaged over 512 cycles (triggered on  $1rf2$  at 50Hz, beaming only at MS/32)

Ch4 (blue): LOI Grid Volts Monitor averaged over 512 cycles (triggered  $1rf2$  at 50Hz, beaming only at MS/32)

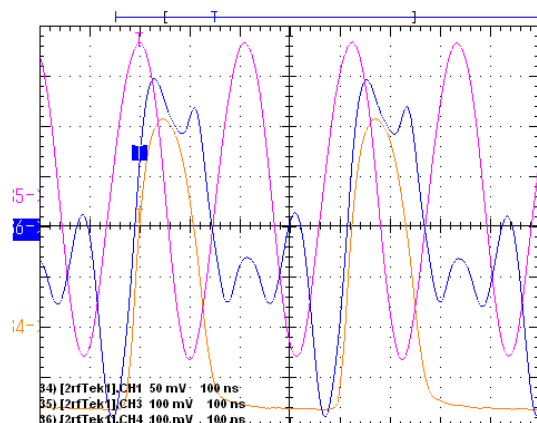


Fig. 10: LOI operation at 5.6kV using old MO. Beam on.  $2.54 \times 10^{13}$  injected,  $2.40 \times 10^{13}$  accelerated (99% acc. efficiency on good pulse!), B triggered at 4.182ms after field minimum.

Ch1 (ocher): Beam Pulse Signal

Ch3 (pink): LOI Grid Current Monitor averaged over 512 beam pulses

Ch4 (blue): LOI Grid Volts Monitor averaged over 512 beam pulses

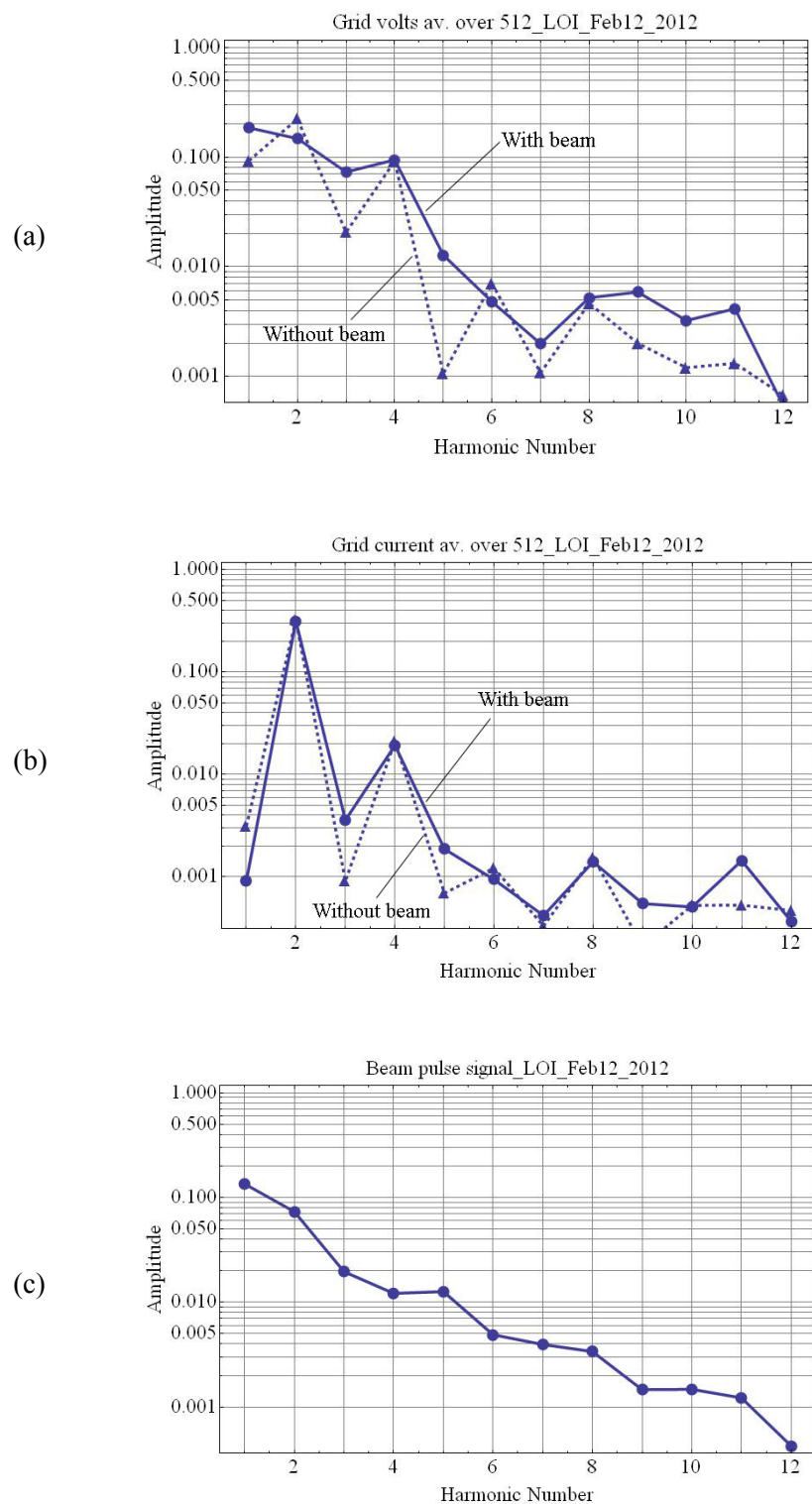


Fig. 11: Harmonic contents of (a) grid voltage, (b) grid input current and (c) beam pulse. at 4.182ms after field minimum. Solid and dashed lines are with beam at  $2.4 \times 10^{13}$  ppp and without beam, respectively.

### 3-3 Spice simulation for waveform distortions

Spice simulation was conducted to reproduce the waveforms in [figs. 9 and 10](#). Firstly, it is assumed that the RF-law signal to the LOI has a subharmonic and higher harmonic

components to simulate the real MO output and the saturation in the subsequent stage [1]. The cavity is assumed to be tuned at 4.71MHz, which is the resonant frequency at 4.18ms after field minimum. Fig. 12 shows the result without beam. Secondly, the beam signal is connected across the LOI cavity gap as a current source, whose component is given in fig. 11(c). The result is shown in fig. 13 in a dashed line. Agreement is not so good with only a beam component. However, it should be reasonable to add another harmonic component at the RF-law signal to take into account further saturations by the beam loading, as is seen in the change of grid input current in fig. 11(b). Also, there possibly is a slight detuning of the cavity. The result including these assumptions is shown in fig. 13 in a blue solid line. Although slight difference is still seen around the large peak, general trend agrees well with the measurements. The parameter used in the calculation is summarized in Table 2.

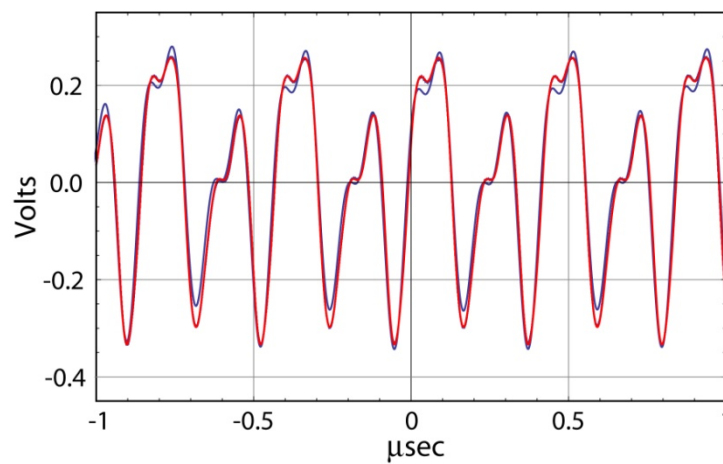


Fig. 12: Comparison of measured (red) and calculated (blue) waveforms of grid voltage without beam.

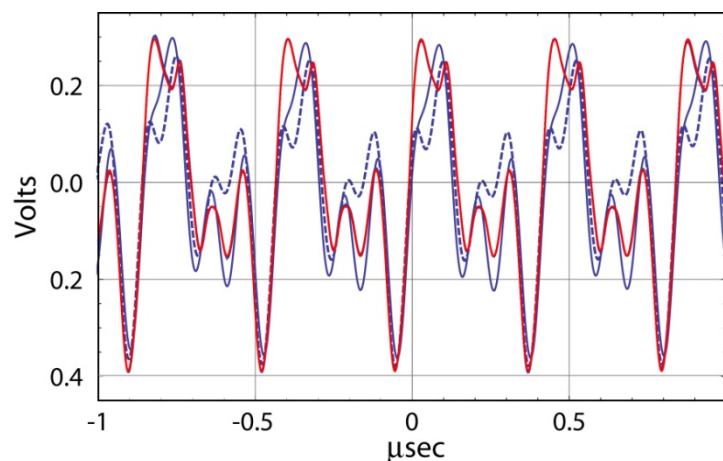


Fig. 13: Comparison of measured (red) and calculated (blue) waveforms of grid voltage with beam.  
See text for details.

Table 2: Harmonic content in the Spice simulation.

Only “RF-law” signal is used for without-beam simulation, while all items are used for with-beam simulation. Cavity inductance is changed from 0.649 $\mu$ H to 0.640 $\mu$ H for detuning.

Harmonic number	RF-law		Further saturation		Beam signal	
	mag.	rad.	mag.	rad.	mag.	rad.
1	0.013	2.54	0.01	-3.36	0.1618	-1.38
2	1.00	-0.2	—		0.0879	-2.13
3	0.03	-0.5	-0.10	-12.0	0.0235	-8.85
4	0.13	-1.2	—		0.0146	-1.22
5	—		—		0.0152	-1.55
6	—		—		0.0059	-1.60
7	—		—		0.0047	-0.75
8	—		—		0.0041	-0.93

### 3-4 Cavity tuning with gap voltage and grid input current

Cavity tuning was tested by using the grid input current to avoid the influence of beam on the PD signal. The results are shown in [figs. 14 and 15](#), where tune correction was not applied. The cavity input current has a sharp minimum at  $\sim 2.3$ ms ( $\sim 3.1$ MHz), and the PD signal between grid input current and gap voltage shows a steep increase around this timing. (Why?) The phase deviation of the PD signal was less than 8 degrees at  $2.54 \times 10^{13}$  ppp intensity. Also, cavity lock signal of the LOI showed very small deviation, although the photo was not taken due to beam stop.

It should be considered whether the grid input current is really usable for fine LOI tuning. It surely is an advantage that the grid input current always has a fine sine waveform no matter how the load changes. However, this fact in turn means the grid input current is insensitive to the cavity conditions, which may not be appropriate for fine tuning. This point will be discussed in section 4.

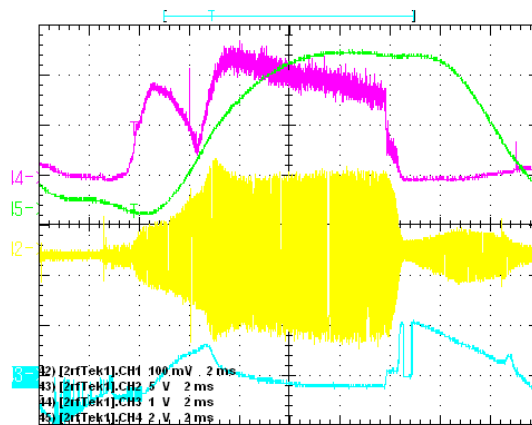


Fig. 14: LOI operation at 2.5kV using old MO. Beam on. 2.54E13 injected, 2.38E13 accelerated. Tuning loop closed with grid input current and gap volts (no offset)

Ch1 (yellow): Grid input current (PD grid volt monitor)

Ch2 (cyan) : LOI cavity tune PD monitor

Ch3 (magenta): LOI cavity input current monitor

Ch4 (green): LOI Bias demand +ve

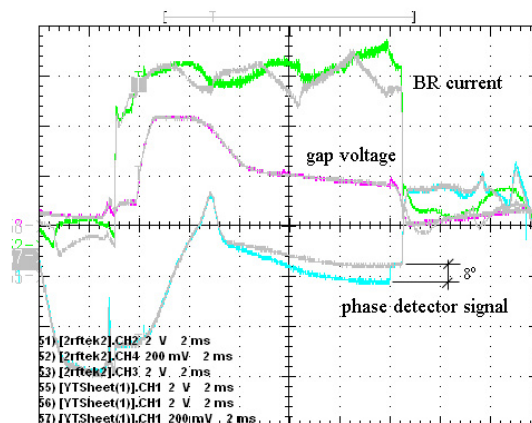


Fig. 15: **Combined Graphics** of "LOI\_Feb13\_2012\_gridcurrent\_tuning\_beam.wk" and "LOI\_Feb13\_2012\_gridcurrent\_tuning\_no\_beam.wk".

LOI operation at 2.5kV using old MO. Beam on. 2.54E13 injected, 2.38E13 accelerated. Tuning loop closed with grid input current and gap volts (no offset)

Ch2: Phase detector signal; grey for no beam case

Ch3: LOI gap volts monitor

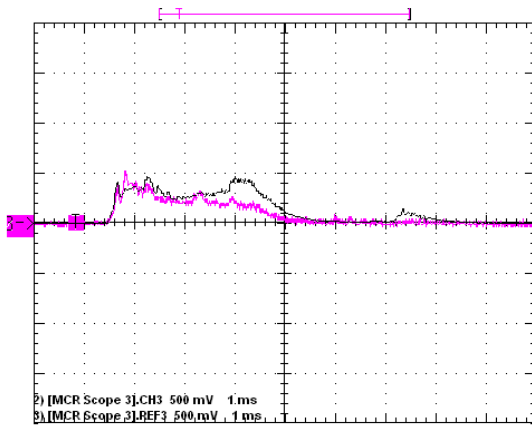
Ch4: LOI BR (buck regulator) current

### 3-5 Preliminary test on the beam loss with LOI

Beam loss was observed by adding the LOI to the operating 2RF5 and 2RF8 systems. The gap voltage envelope of the LOI has a shape of that in [fig. 15](#), and the PD was made using gap and grid voltages. With increasing the gap voltage, it soon took effect on the beam loss.

[Fig.16](#) shows the beam loss signal at  $2.54 \times 10^{13}$  ppp injected beam intensity, where the beam loss signal is the sum output of the beam loss monitors (BLM) surrounding the ISIS

synchrotron. The beam loss became almost half of the reference at  $\sim 3$ ms after field minimum when the gap voltage was 5.4 kVp. Also, trapping efficiency, which is defined as the ratio of the survived beam intensity at 2.5ms to the injected one, reached 99% occasionally.



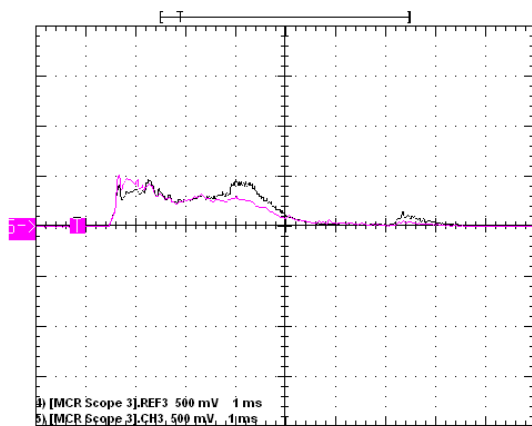
#### LOI-Feb11-2012-2.wk

LOI With beam tests 1.6Hz rep rate  $2.54 \times 10^{13}$  injected,  $2.39 \times 10^{13}$  accelerated (good pulse).

Beam Loss Sum Monitor signal

Ch3 (pink): Good pulse with LOI on, 5.4kV peak gapvolts

Ref 3 (black): Typical BLM without LOI.



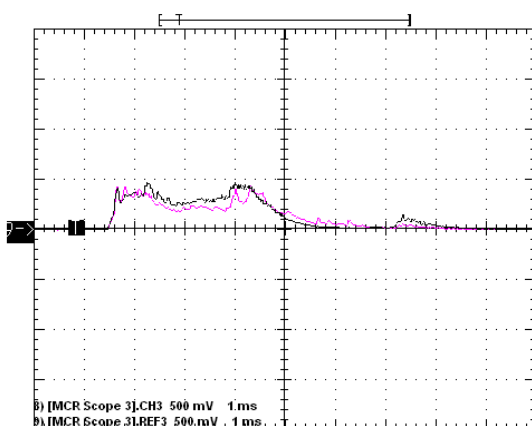
#### LOI-Feb11-2012-5.wk

LOI With beam tests 1.6Hz rep rate  $2.54 \times 10^{13}$  injected,  $2.39 \times 10^{13}$  accelerated (good pulse).

Beam Loss Sum Monitor signal averaged over 32 pulses

Ch3 (pink): Good pulse with LOI on, 7.2kV peak gapvolts

Ref 3 (black): Typical BLM without LOI.



#### LOI-Feb11-2012-7.wk

LOI With beam tests 1.6Hz rep rate  $2.54 \times 10^{13}$  injected,  $2.39 \times 10^{13}$  accelerated (good pulse

$\sim 99\%$  acc efficiency!). Beam Loss Sum

Monitor signal averaged over 32 pulses

Ch3 (pink): Good pulse with LOI on, 6.7kV peak gapvolts (gapvolts demand held on to 2.7ms, as per 2012\_6)

Ref 3 (black): Typical BLM without LOI.

Fig. 16: Beam loss signal with LOI: 2RF5 and 8 are in simultaneous operation.

## 4. Sensitivity Analysis

An AC analysis using the TopSpice simulation code was performed to investigate the tuning sensitivity of the phase difference ( $\Delta\phi$ ) upon frequency, where  $\Delta\phi$  is between grid and cavity voltages ( $\Delta\phi_{gv}$ ) or between grid input current and cavity voltage ( $\Delta\phi_{gc}$ ). The frequency was scanned over the resonances where the cavity is on tune, or the triode output current is minimum. The tuning sensitivity is defined as the ratio of frequency variation of  $\Delta\phi$  to the frequency span at resonance as illustrated in fig.17. Fig. 18 shows the result of simulation. It is seen  $\Delta\phi_{gv}$  is much sensitive to frequency error than  $\Delta\phi_{gc}$  for both resonant cases. From view point of the limited available power, however, the condition for minimum triode current is preferable rather than that for minimum cavity input current [2].

Therefore, we think it is better to use the grid voltage signal for fine LOI tuning. In order to eliminate the subharmonic distortions, the variable bandpass filter [2] should be used at the input of phase detector for cavity tuning. The same filter is used for the cavity voltage signal to equalize the delay time with the grid voltage signal.

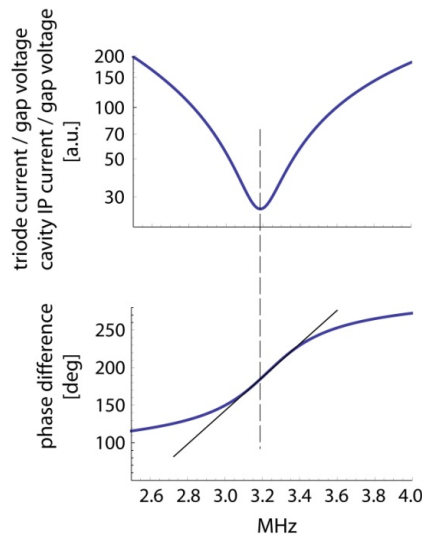


Fig. 17: Definition of tuning sensitivity. It is defined as the gradient of tangent at the resonance in the lower figure.

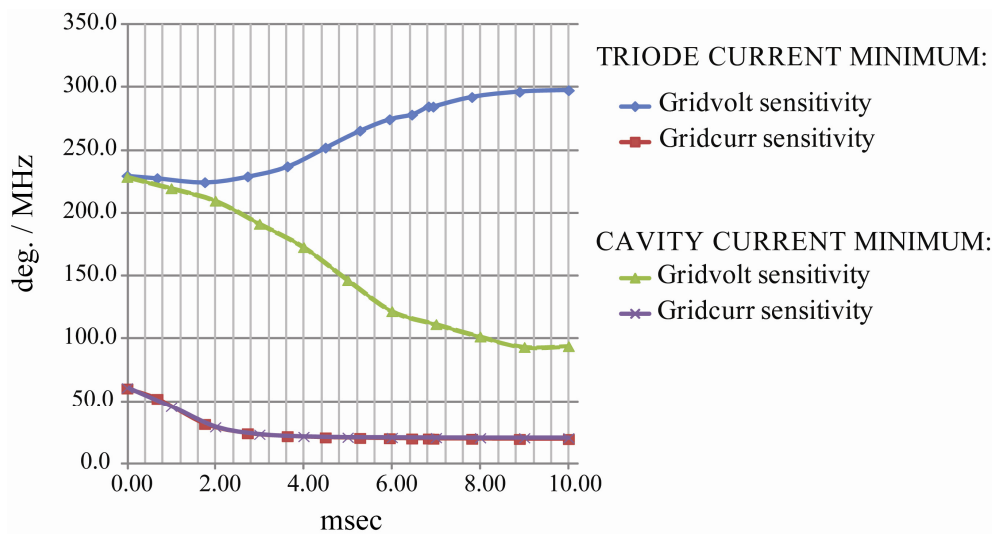


Fig. 18: Comparison of the tuning sensitivity between minimum triode current and minimum cavity current conditions. Phase difference of grid and cavity voltages is much sensitive for both cases.

## 5. Faults

During starting up of the LOI system, buck regulator (BR) was tripped, showing “trip” alert at the opening module (A3). However, it could not be reset. The needle of the output voltage meter at A3 pointed far less than zero, and an analog output for the BR output voltage showed a saw-tooth waveform at  $\sim 1.56\text{Hz}$  (fig. 19). DC voltage of the A3 was tested for  $-5\text{V}$  and  $\mp 15\text{V}$ , and they showed OK. Although no repair had been made, the alert became possible to be reset (Why?)

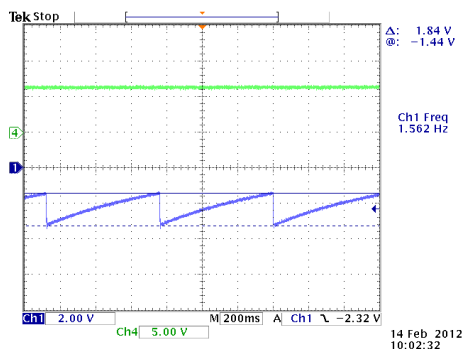


Fig. 19: Anode voltage monitor output. Blue line is for BR. Saw-tooth waveform ranges from  $-1.44\text{V}$  to  $-3.28\text{V}$  at  $1.56\text{Hz}$ . (green line is for driver supply voltage).

## 6. Discussions & conclusions

The grid voltage and grid input current have been studied on either of which is suitable for the LOI tuning. The grid voltage waveform is easily distorted by a small content of harmonics in the master oscillator as well as the beam current. On the other hand, grid input current waveform is hardly affected by those effects. However, from view point of tuning sensitivity, it is shown by the Spice simulation that the phase between grid and cavity voltages is much sensitive to the tuning error by more than a factor of 4 than that for the grid input current and cavity voltage. Thus, we can conclude the grid voltage is suitable for efficient tuning rather than the grid input current. In order to eliminate the phase error caused by waveform distortions, a variable bandpass filter is necessary for both signals at the input of phase detector.

Cleaning effort has been made to eliminate unnecessary harmonic components in the master oscillator output, and it succeeded to produce a fine sine waveform at the grid voltage. However, it was found that even a fine waveform is strongly distorted eventually by the beam.

### References:

- [1] LOI progress report LOI-8, September 13, 2010.
- [2] LOI progress report LOI-12, August 29, 2011.